ARTICLE

The SKI proto-oncogene restrains the resident CD103$^+$CD8$^+$ T cell response in viral clearance

Bing Wu[1,2], Ge Zhang[1,2,3], Zengli Guo[1,2], Gang Wang[1,2,4], Xiaojiang Xu[5], Jian-liang Li[5], Jason K. Whitmire[1,2,6], Junnian Zheng[4] and Yisong Y. Wan[1,2]

Acute viral infection causes illness and death. In addition, an infection often results in increased susceptibility to a secondary infection, but the mechanisms behind this susceptibility are poorly understood. Since its initial identification as a marker for resident memory CD8$^+$ T cells in barrier tissues, the function and regulation of CD103 integrin (encoded by *ITGAE* gene) have been extensively investigated. Nonetheless, the function and regulation of the resident CD103$^+$CD8$^+$ T cell response to acute viral infection remain unclear. Although TGFβ signaling is essential for CD103 expression, the precise molecular mechanism behind this regulation is elusive. Here, we reveal a TGFβ–SKI–Smad4 pathway that critically and specifically directs resident CD103$^+$CD8$^+$ T cell generation for protective immunity against primary and secondary viral infection. We found that resident CD103$^+$CD8$^+$ T cells are abundant in both lymphoid and nonlymphoid tissues from uninfected mice. CD103 acts as a costimulation signal to produce an optimal antigenic CD8$^+$ T cell response to acute viral infection. There is a reduction in resident CD103$^+$CD8$^+$ T cells following primary infection that results in increased susceptibility of the host to secondary infection. Intriguingly, CD103 expression inversely and specifically correlates with SKI proto-oncogene (SKI) expression but not R-Smad2/3 activation. Ectopic expression of SKI restricts CD103 expression in CD8$^+$ T cells in vitro and in vivo to hamper viral clearance. Mechanistically, SKI is recruited to the *Itgae* loci to directly suppress CD103 transcription by regulating histone acetylation in a Smad4-dependent manner. Our study therefore reveals that resident CD103$^+$CD8$^+$ T cells dictate protective immunity during primary and secondary infection. Interfering with SKI function may amplify the resident CD103$^+$CD8$^+$ T cell response to promote protective immunity.

Keywords: CD103; TGFβ; SKI; Smad4; LCMV infection; Histone acetylation

Cellular & Molecular Immunology (2021) 18:2410–2421; https://doi.org/10.1038/s41423-020-0495-7

INTRODUCTION

Pathogenic infection has afflicted mankind throughout history. A common complication during acute viral infection is increased susceptibility to secondary infection morbidity and mortality.[1–3] Multiple factors, including epithelial cell damage and innate immune dysfunction, contribute to the susceptibility to secondary infections.[4,5] Nonetheless, whether and how adaptive immunity and its effectors, especially CD8$^+$ T cells, are involved is poorly understood.

CD8$^+$ T cells are critical for clearing infected and transformed cells because they mount effective primary and memory responses.[6,7] Based on the expression of different surface markers, CD8$^+$ T cells can be categorized into various subsets.[8] In particular, CD103 was initially identified as a hallmark of tissue-resident memory (Trm) CD8$^+$ T cells that contributed to Trm CD8$^+$ T cell function.[9] Encoded by the *Itgae* gene, CD103 is the αE subunit of the heterodimeric integrin αEβ7.[10] CD103 binds to its receptor E-cadherin on target tissue cells to facilitate the tissue migration and retention of Trm CD8$^+$ T cells in barrier tissues.[11] Nonetheless, emerging evidence suggests that CD103 expression is not restricted to memory CD8$^+$ T cells in nonlymphoid tissues[12] and that CD103 may regulate diverse immune cell functions in a microenvironment-dependent fashion.[5,13–17] In addition, CD103 can promote the cytotoxic killing activity of CD8$^+$ T cells and increase TCR antigen sensitivity.[18–22] This evidence suggests that CD103 plays a broad role in CD8$^+$ T cell immunity beyond regulating the resident memory response. However, the regulation and function of resident CD103$^+$CD8$^+$ T cells during acute viral infection remain ill defined.

Therefore, the expression of CD103 is controlled is a question of significance that is under intense investigation.[23,24] Transforming growth factor-beta (TGFβ) signaling is vital for CD103 expression.[25–27] The binding of TGFβ to its receptors, including TGFβRI and TGFβRII, leads to the phosphorylation and activation of receptor-associated Smad2/3 (R-Smad2/3).[28] TGFβ induces the degradation of the SKI pro-oncogene and, as such, it negatively

[1]Lineberger Comprehensive Cancer Center, School of Medicine, University of North Carolina at Chapel Hill, Chapel Hill, NC 27599, USA; [2]Department of Microbiology and Immunology, School of Medicine, University of North Carolina at Chapel Hill, Chapel Hill, NC 27599, USA; [3]Department of Immunology, College of Basic Medical Science, Dalian Medical University, Dalian, Liaoning 116044, China; [4]Jiangsu Center for the Collaboration and Innovation of Cancer Biotherapy, Cancer Institute, Xuzhou Medical University, Xuzhou, Jiangsu 221002, China; [5]Integrative Bioinformatics, National Institute of Environmental Health Sciences, Research Triangle Park, Chapel Hill, NC 27709, USA and [6]Department of Genetics, School of Medicine, University of North Carolina at Chapel Hill, Chapel Hill, NC 27599, USA
Correspondence: Junnian Zheng (jnzheng@xzhmu.edu.cn) or Yisong Y. Wan (wany@email.unc.edu)
These authors contributed equally: Bing Wu, Ge Zhang

Received: 18 March 2020 Accepted: 13 June 2020
Published online: 1 July 2020

regulates TGFβ signaling.[29] Both R-Smad2/3 and SKI can bind to Smad4 to control target gene expression.[28,30] Although TGFβR and R-Smad2/3 have been shown to be required for CD103 expression,[25,27] whether and how SKI and Smad4 control CD103 expression remains unaddressed to date. More importantly, because interfering with TGFβR and R-Smad2/3 often leads to unwanted global effects beyond CD103 function because of their broad and pleiotropic functions, it is of interest to identify factors and pathways that specifically control CD103 expression and function.

Lymphocytic choriomeningitis virus (LCMV) is a prevalent human pathogen that infects a large number of people.[31] Infection of mice with LCMV can be used to study the underlying principles of viral infection and immune response.[32] Using mouse LCMV infection models, we discovered that the TGFβ–SKI–Smad4 pathway is critical in directing $CD103^+CD8^+$ T cell generation to fight against primary and secondary infection. We found that the resident $CD103^+CD8^+$ T cell population was abundant in nonpathogen-experienced mice, but it changed dynamically after viral infection. Mice with a reduced $CD103^+CD8^+$ T cell population were more susceptible to secondary infection. In addition, CD103 expression on $CD8^+$ T cells was found to act as a costimulatory signal for the primary T cell response against acute viral infection. Interestingly, CD103 expression specifically and inversely correlated with SKI expression but not R-Smad activation. Ectopic expression of SKI restricted $CD103^+CD8^+$ T cells in vitro and in vivo to hamper viral clearance. In addition, we found that Smad4 was required for the suppression of CD103 expression because CD103 was constitutively expressed in the absence of Smad4 even when TGFβ signaling was abrogated. Furthermore, SKI co-opted Smad4 to restrain CD103 expression by directly binding to the *Itgae* loci and suppressing CD103 transcription through the inhibition of histone acetylation.

RESULTS

Resident $CD103^+CD8^+$ T cells contribute to the control of primary and secondary LCMV infection

To understand the contribution of resident $CD103^+CD8^+$ T cells to immune defense, we examined the temporal change in CD103 expression in $CD8^+$ T cells in different tissues before and after viral infection. Appreciable fractions of $CD103^+CD8^+$ T cells were identified in both lymphoid and nonlymphoid tissues in pathogen-naive mice (Figs. 1a and S1a–c), which was in agreement with previous reports and suggested a broad role of CD103 in immunity.[33–35] Upon acute LCMV Armstrong strain infection,[36] resident $CD103^+CD8^+$ T cell population declined dramatically and reached their lowest levels ~7 days after infection; this was followed by a gradual recovery of cell numbers, as indicated at both the protein and mRNA levels at day 35 post infection when the memory response was initiated (Figs. 1a, b and S1a–c). Such a dynamic change in the $CD103^+CD8^+$ T cell population suggests that these cells play a role in the acute antiviral response.

It is noteworthy that re-exposure to LCMV infection 7 days after the first infection, when $CD103^+CD8^+$ T cells were at low levels, led to animal death (Fig. 1c), decline in body weight (Fig. 1d), and reduced pathogen clearance (Fig. 1e), suggesting a protective role of $CD103^+CD8^+$ T cells during secondary infection. Importantly, antibody-mediated blocking of CD103 (Fig. S1d) led to similar animal death (Fig. 1f), decline in body weight (Fig. 1g), and reduced viral clearance (Fig. 1h) upon LCMV infection. In addition, the virus-specific, GP33/H2-D^b tetramer-positive[37] $CD8^+$ T cell population was substantially reduced in mice pretreated with an anti-CD103 antibody (Figs. 1i and S1e), although antibody treatment itself did not perturb the $CD8^+$ T cell population (Fig. S1f). Thus, CD103 acts as a costimulation signal to ready $CD8^+$ T cells for an optimal response to acute primary and secondary infection. Furthermore, we found that anti-CD103 antibody-treated mice that were also transplanted with $CD103^+CD8^+$ T cells (Fig. S1g, h) were more protected than those that were transplanted with $CD103^-CD8^+$ T cells (Fig. 1j, k). These results therefore suggest that reduced resident $CD103^+CD8^+$ T cell numbers result in increased susceptibility to secondary infection and that CD103 expression is important for $CD8^+$ T cells to respond to and clear viral infection.

TGFβ signaling is critical for the induction and maintenance of CD103 expression

We next investigated how CD103 expression is regulated in $CD8^+$ T cells. TGFβ signaling is required for the development of resident memory $CD103^+CD8^+$ cells in barrier tissues.[25,38] Similarly, we found that the deletion of TGFβRII[39] abrogated the $CD103^+CD8^+$ T cell population in both lymphoid and nonlymphoid tissues of *Cd4Cre;Tgfbr2$^{fl/fl}$* mice, suggesting an essential role of TGFβR signaling in regulating CD103 expression during homeostasis (Figs. 2a and S2a). In addition, by culturing purified $CD103^+CD8^+$ T cells in the presence or absence of TGFβ, we found that TGFβ promoted the maintenance of CD103 expression on $CD8^+$ T cells in vitro (Figs. 2b and S2b). Moreover, low doses of TGFβ induced de novo CD103 expression in activated $CD103^-CD8^+$ T cells in vitro (Figs. 2c and S2c). These findings underscore a central role for TGFβ signaling in inducing and maintaining CD103 expression in vivo and in vitro.

SKI expression inversely correlates with CD103 expression in $CD8^+$ T cells

Intriguingly, we consistently observed that only a portion of $CD8^+$ T cells expressed CD103 following TGFβ stimulation (Fig. 2c). Such observation could be attributed to a difference in the downstream signaling of TGFβR in $CD103^+$ vs. $CD103^-$ $CD8^+$ T cells. To address this, the phosphorylation levels of R-Smad2 and R-Smad3 were first determined in $CD103^+$ vs. $CD103^-$ $CD8^+$ T cells. Of note, TGFβ induced comparable phosphorylation of R-Smad2 and R-Smad3 in $CD103^+$ and $CD103^-$ $CD8^+$ T cells in vitro (Fig. 3a, b). Of interest, TGFβ-induced much more SKI degradation (Fig. S3a) in $CD103^+$ than in $CD103^-$ $CD8^+$ T cells in vitro (Fig. 3a, b). Similarly, SKI protein expression inversely correlated with CD103 expression in $CD8^+$ T cells from mice during the course of LCMV infection, although the phosphorylation of R-Smad2 and R-Smad3 did not fluctuate (Fig. 3c, d). Mirroring what was observed in vitro, $CD103^+CD8^+$ T cells expressed much lower levels of SKI than their $CD103^-CD8^+$ counterparts in uninfected and LCMV-infected mice, while the phosphorylation of R-Smad2 and R-Smad3 appeared comparable (Fig. 3e). The consistent inverse correlation between SKI and CD103 expression strongly suggested a specific role for SKI in restricting CD103 expression. Indeed, retrovirus-mediated ectopic SKI expression potently suppressed the promotion of CD103 expression in $CD8^+$ T cells by TGFβ at both the protein and mRNA levels (Figs. 3f and S3b). These findings suggest that TGFβ-induced SKI downregulation, but not R-Smad2/3 activation, specifically directs CD103 expression in $CD8^+$ T cells.

SKI suppresses resident $CD103^+CD8^+$ T cells to hamper antiviral responses

To further investigate the role of SKI in controlling resident $CD103^+CD8^+$ T cell-mediated antiviral function in vivo, we generated a mouse strain in which a Cre recombinase-inducible SKI expression cassette was knocked into the *Rosa26* locus (*Rosa26-iSki* strain) (Fig. S4a). By crossing *Rosa26-iSki* with *Cd4Cre*[40] mice, we ectopically expressed SKI in T cells in vivo (Fig. S4b). Although SKI has been suggested to inhibit TGFβ signaling,[41] *Cd4Cre;Rosa26-iSki* (*SKI-KI*) mice were grossly normal, unlike mice whose T cells are deficient in TGFβR or R-Smad2/3.[27,42–45] The homeostasis of $CD4^+$ and $CD8^+$ T cells in the

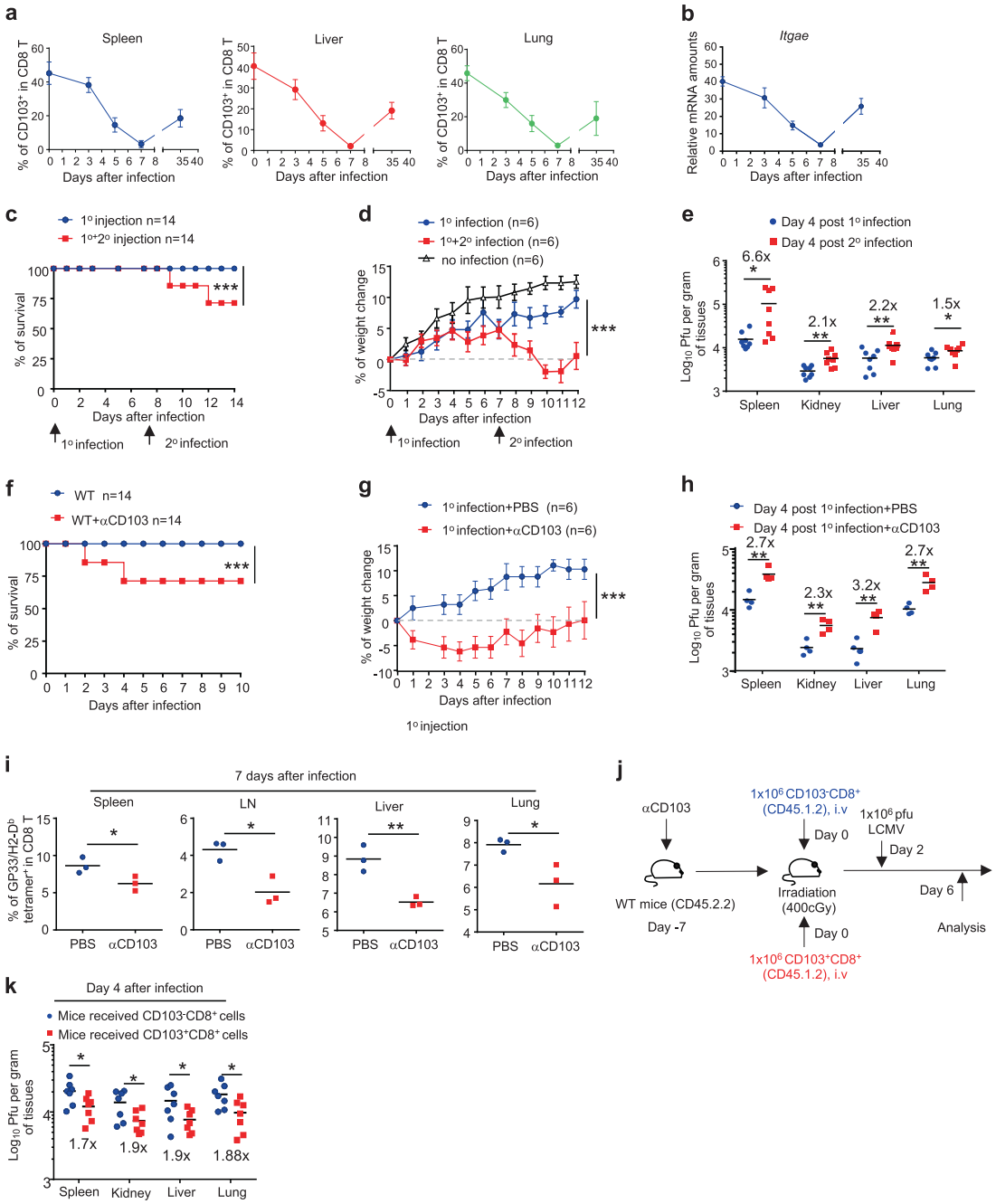

Fig. 1 The distribution, dynamics, and function of resident CD103$^+$CD8$^+$ T cells during LCMV-Armstrong infection. **a** Flow cytometry analysis of CD103$^+$CD8$^+$ T cells in the spleen (blue), liver (red), and lung (green) from wild-type (WT) mice at different time points after infection with LCMV-Armstrong. (the mean ± s.d.; $n = 3$–4 mice of three experiments). **b** *Itgae* mRNA expression in splenic CD8$^+$ T cells isolated from LCMV-Armstrong-infected WT mice at the indicated time points, assayed by qRT-PCR. (the mean ± s.d; $n = 3$ experiments). **c**–**e** WT mice were infected with LCMV-Armstrong once (1°) or twice (2°) as indicated. The survival (**c**), body weight change (**d**), and viral titers in different tissues (**e**) were determined at the indicated time points. Organ samples were collected either at day 4 post 1st injection or 4 days after the 2nd infection (11 days post 1st infection). ($n = 14$ mice of two experiments for **c**; $n = 6$ mice of three experiments for (**d**); the mean ± s.e.m. for (**d**); $n = 8$ from three experiments for **e**; ***$p < 0.001$ per two-way multiple-range ANOVA test for (**c**) and (**d**); *$p < 0.05$, and **$p < 0.01$ two-sided *t*-test for (**e**), centers indicate the mean values). **f**–**h** Mice were injected with 500 μg of anti-CD103 (αCD103) or with control PBS 3 days before they were infected once with LCMV-Armstrong. The survival rate (**f**), body weight change (**g**), and viral titers in different tissues (**h**) were monitored at the indicated time points. ($n = 14$ mice of two experiments for (**h**); $n = 6$ mice of three experiments for (**g**), $n = 4$ mice of two experiments for (**h**). The mean ± s.e.m. for (**g**); ***$p < 0.001$ per two-way multiple-range ANOVA test for (**f**) and (**g**); **$p < 0.01$ per two-sided t-test for (**h**); centers indicate the mean values). **i** The percentages of LCMV antigen-specific CD8$^+$ T cells identified by LCMV-GP33/H2-D^b tetramer staining in different tissues from LCMV-infected mice that were treated with αCD103 or PBS for 3 days prior to LCMV infection. ($n = 3$ mice of two experiments; *$p < 0.05$, and **$p < 0.01$ per two-sided *t*-test; centers indicate the mean values). **j** The experimental design of intravenous (i.v.) transfer of purified CD103$^-$CD8$^+$ T cells and CD103$^+$CD8$^+$ T cells (CD45.1$^+$CD45.2$^+$) into αCD103 pretreated and irradiated WT (CD45.2$^+$) mice, which was followed by LCMV-Armstrong infection for (**k**) and Fig. S1g, h. **k** Viral titer in different tissues from recipient mice 4 days post LCMV-Armstrong infection as depicted in (**j**). ($n = 7$ mice of two experiments; *$p < 0.05$, per two-sided *t*-test; centers indicate the mean values)

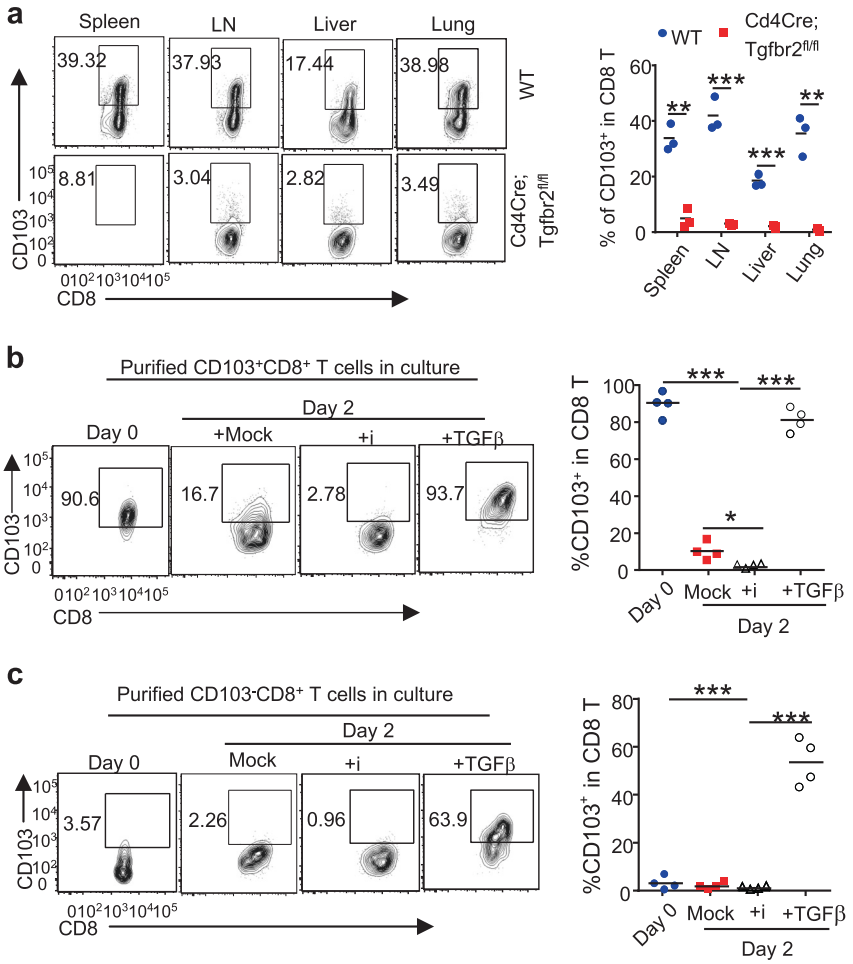

Fig. 2 TGFβ is important for the induction and maintenance of CD103 expression in $CD8^+$ T cells. **a** Flow cytometry of $CD103^+CD8^+$ T cells in different tissues from mice of the indicated genotypes. ($n = 3$ mice of three experiments; representative results are shown; $^{**}p < 0.01$, and $^{***}p < 0.001$, per two-sided *t*-test; centers indicate the mean values). Flow cytometry of CD103 expression in purified $CD103^+CD8^+$ (**b**) or $CD103^-CD8^+$ (**c**) T cells after being activated in the absence (mock) or presence of TGFβR inhibitor (SB525334, i) or 0.25 ng/ml TGFβ for the indicated time. ($n = 4$ samples of three experiments; $^{***}p < 0.001$ per two-sided *t*-test; centers indicate the mean values)

periphery of these mice was largely unperturbed, although the $CD8^+$ T cell population was slightly reduced in the spleen and lymph nodes (Fig. S4c, d). In addition, although SKI negatively regulates TGFβ signaling,[30] the development of regulatory T cells remained undisturbed in *SKI-KI* mice (Fig. S4e). The normal phenotype of *SKI-KI* mice under steady state therefore allowed us to investigate how SKI specifically controls CD103 expression and function.

Consistent with the findings that retrovirus-mediated SKI expression suppressed CD103 expression in $CD8^+$ T cells in vitro (Figs. 3f and S3b), $CD8^+$ T cells from *SKI-KI* mice were defective in gaining CD103 expression upon TGFβ stimulation in vitro (Fig. 4a, b). Importantly, resident $CD103^+CD8^+$ T cell populations were greatly reduced in both lymphoid and nonlymphoid tissues from *SKI-KI* mice (Fig. 4c, d). By infecting *SKI-KI* mice with the LCMV-Armstrong virus, we assessed how SKI expression could impact host resistance to viral infection. We found that, unlike wild-type mice, *SKI-KI* mice cleared viruses poorly (Fig. 4e) and lost weight upon acute LCMV infection (Fig. 4f), which was associated with impaired expansion of LCMV-specific GP33/H2-D^b tetramer-positive $CD8^+$ T cells (Fig. 4g). In addition, the ability of *SKI-KI* mice to generate memory $CD103^+CD8^+$ T cells following viral clearance was also impaired, and this effect was most severe in the nonlymphoid tissues (Fig. 4h). These findings suggest that TGFβ-induced SKI downregulation is critical for enabling the generation of resident $CD103^+CD8^+$ T cells to fight against infection.

SKI interacts with Smad4, which is required to suppress CD103 expression in $CD8^+$ T cells

We found that CD103 mRNA *(Itgae)* expression virtually mirrored its protein expression under various in vivo and in vitro conditions (Figs. 1a, b, 2a–c, and S2a–c), and this expression was suppressed by SKI (Figs. 3f, 4a–d, and S3b), indicating that SKI regulates CD103 expression at the transcriptional level. Although SKI is not a transcription factor, it controls the expression of diverse genes by binding to transcription factors.[30] SKI associates with the transcription factor Smad4 to control gene expression.[46] To confirm this observation, we found that SKI bound to Smad4 in $CD8^+$ T cells by immunoprecipitation (IP) (Fig. 5a), suggesting a role for Smad4 in controlling CD103 expression. To address whether and how Smad4 is required for the generation of resident $CD103^+CD8^+$ T cells, we investigated CD103 expression in $CD8^+$ T cells of *Cd4Cre;Smad4*$^{fl/fl}$ mice.[47] We found that Smad4 deficiency led to a consistent increase of the resident $CD103^+CD8^+$ T cell population in the lymphoid and nonlymphoid tissues of *Cd4Cre;Smad4*$^{fl/fl}$ mice when they remained uninfected or during the course of LCMV-Armstrong infection and reinfection (Figs. 5b–d and S5a–e). In addition, Smad4 deletion led to increased virus-specific GP33/H2-D^b tetramer-positive $CD8^+$ T cells

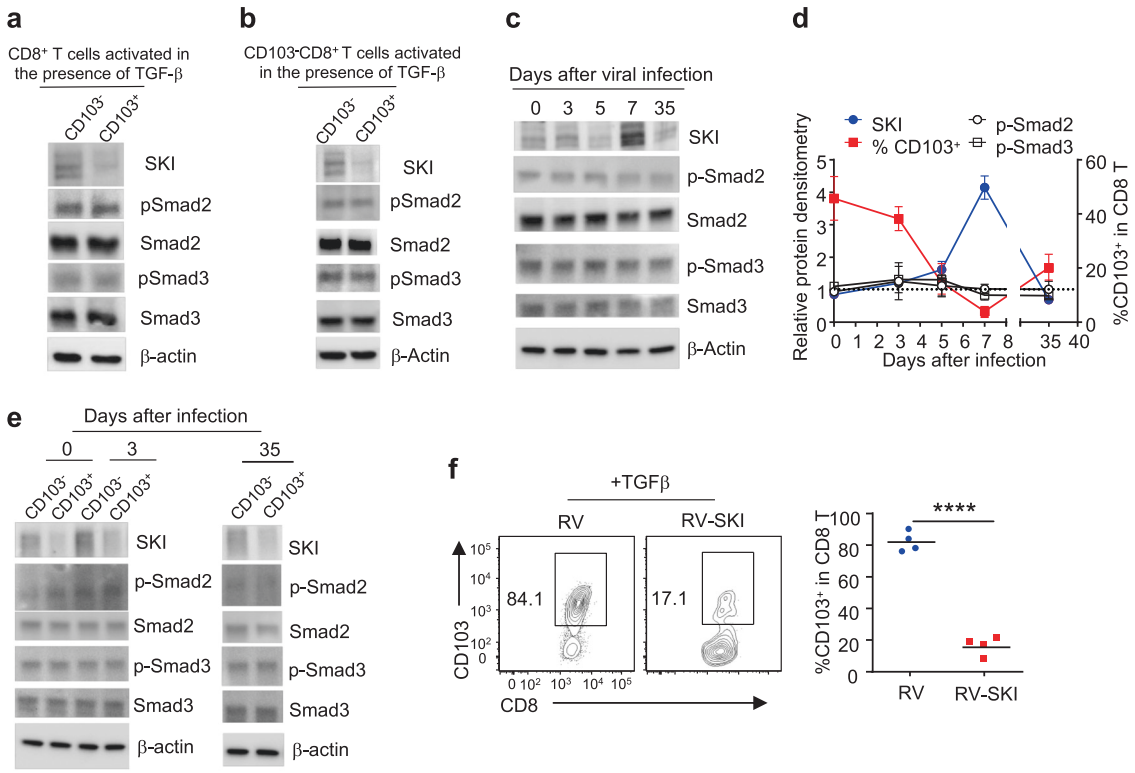

Fig. 3 SKI expression inversely correlates with CD103 expression in CD8$^+$ T cells both in vitro and in vivo. Immunoblotting of SKI, phospho-Smad2 (p-Smad2), Smad2, phospho-Smad3 (p-Smad3), and Smad3 in purified CD103$^+$CD8$^+$ and CD103$^-$CD8$^+$ T cells after total CD8$^+$ (**a**) and CD103$^-$CD8$^+$ (**b**) T cells were activated for 2 days in the presence of 0.25 ng/ml TGFβ. The results are representative of three experiments. **c** Immunoblotting of SKI, phospho-Smad2 (p-Smad2), Smad2, phospho-Smad3 (p-Smad3), and Smad3 in splenic CD8$^+$ T cells from LCMV-infected mice at the indicated time points. The results are representative of three experiments. **d** The comparison between the protein levels of SKI, p-Smad2 and p-Smad3 and CD103 expression in CD8$^+$ T cells after LCMV-Armstrong infection at the indicated time points. (the mean ± s.d. of three experiments). **e** Immunoblotting of SKI, phospho-Smad2 (p-Smad2), Smad2, phospho-Smad3 (p-Smad3), and Smad3 in purified splenic CD103$^+$CD8$^+$ and CD103$^-$CD8$^+$ T cells at the indicated time points after LCMV-Armstrong infection. The results are representative of three experiments. **f** Purified CD8$^+$ T cells were activated in the presence of TGFβ and then transduced with MSCV-IRES-Thy1.1 (RV) or MSCV-SKI-IRES-Thy1.1 (RV-SKI). CD103 expression in transduced (Thy1.1$^+$) cells was detected by flow cytometry 6 days after activation. (n = 4 samples from three experiments; representative results are shown; ****$p < 0.0001$ per two-sided t-test; centers indicate the mean values)

following acute LCMV infection (Figs. 5e and S5f). Furthermore, compared with wild-type mice, *Cd4Cre;Smad4*$^{fl/fl}$ mice were more resistant to LCMV re-exposure-associated animal death (Fig. 5f), body weight decline (Fig. 5g), and unabated virus titer (Fig. 5h). Resident CD103$^+$CD8$^+$ T cells are important for the enhanced antiviral response observed in *Cd4Cre;Smad4*$^{fl/fl}$ mice because antibody-mediated CD103 inhibition (Fig. 5i) neutralized the enhanced ability of *Cd4Cre;Smad4*$^{fl/fl}$ mice to deal with LCMV infection (Fig. 5j, k).

We further assessed how Smad4 is involved in TGFβ-promoted CD103 expression. Interestingly, we found that Smad4 deletion enabled CD103 expression in CD8$^+$ T cells even when TGFβ signaling was abrogated in vitro (Fig. 5l). Consistently, simultaneous deletion of Smad4 restored the CD103$^+$CD8$^+$ T cell population in both lymphoid and nonlymphoid organs from *Cd4Cre;Tgfbr2*$^{fl/fl}$ mice (Figs. 5m and S5g). Therefore, Smad4 is required to limit CD103 expression in CD8$^+$ T cells through a mechanism that is downstream of TGFβR.

SKI co-opts Smad4 to directly suppress CD103 expression by inhibiting histone acetylation

Intrigued by the findings described above, we further investigated the functional relationship of SKI and Smad4 in regulating CD103 expression. We found that ectopic SKI expression suppressed TGFβ-induced CD103 expression only when Smad4 was coexpressed in activated CD8$^+$ T cells in vitro (Fig. 6a). In addition, Smad4 deletion restored the CD103$^+$CD8$^+$ T cell population in *SKI-KI* mice (Fig. 6b). Therefore, SKI suppresses CD103 expression through a Smad4-dependent mechanism. Further investigation revealed that such a mechanism involved the direct binding of the SKI–Smad4 complex to *Itgae* loci. Chromatin immunoprecipitation followed by sequencing (ChIP-seq) (Fig. 6c, e) as well as ChIP analysis (Fig. 6d, f) performed on CD8$^+$ T cells revealed that both Smad4 and SKI bound to the *Itgae* loci containing Smad consensus sites. SKI failed to bind to *Itgae* loci when Smad4 was absent (Fig. 6g), although Smad4 bound to *Itgae* loci constitutively regardless of TGFβ signaling (Fig. 6h), suggesting that SKI is recruited to *Itgae* loci in a Smad4-dependent manner.

Since SKI may control target gene expression by modifying histone acetylation,[30,46] we wondered how TGFβ–SKI–Smad4 signaling impacts the status of H3K9Ac, an epigenetic marker for transcriptional activation,[48] of *Itgae* loci. We found that despite TGFβ treatment, very low levels of H3K9Ac were detected at *Itgae* loci in CD103$^-$CD8$^+$ T cells (Fig. 6i), which expressed high levels of SKI (Fig. 3a, b, e). In contrast, high levels of H3K9Ac were detected at *Itgae* loci in CD103$^+$CD8$^+$ T cells (Fig. 6i), which expressed low levels of SKI (Fig. 3a, b, e). In addition, in the absence of Smad4, SKI failed to be recruited to *Itgae* loci (Fig. 6g), and H3K9Ac was observed at high levels at *Itgae* loci to allow unconstrained CD103 expression in CD8$^+$ T cells (Fig. 6j). Moreover, ectopic SKI expression suppressed H3K9Ac levels at the *Itgae* loci in CD8$^+$ T cells (Fig. 6k). These findings therefore suggest that the SKI–Smad4 complex directly binds to *Itgae* loci to prevent H3K9Ac deposition and restrain CD103 expression.

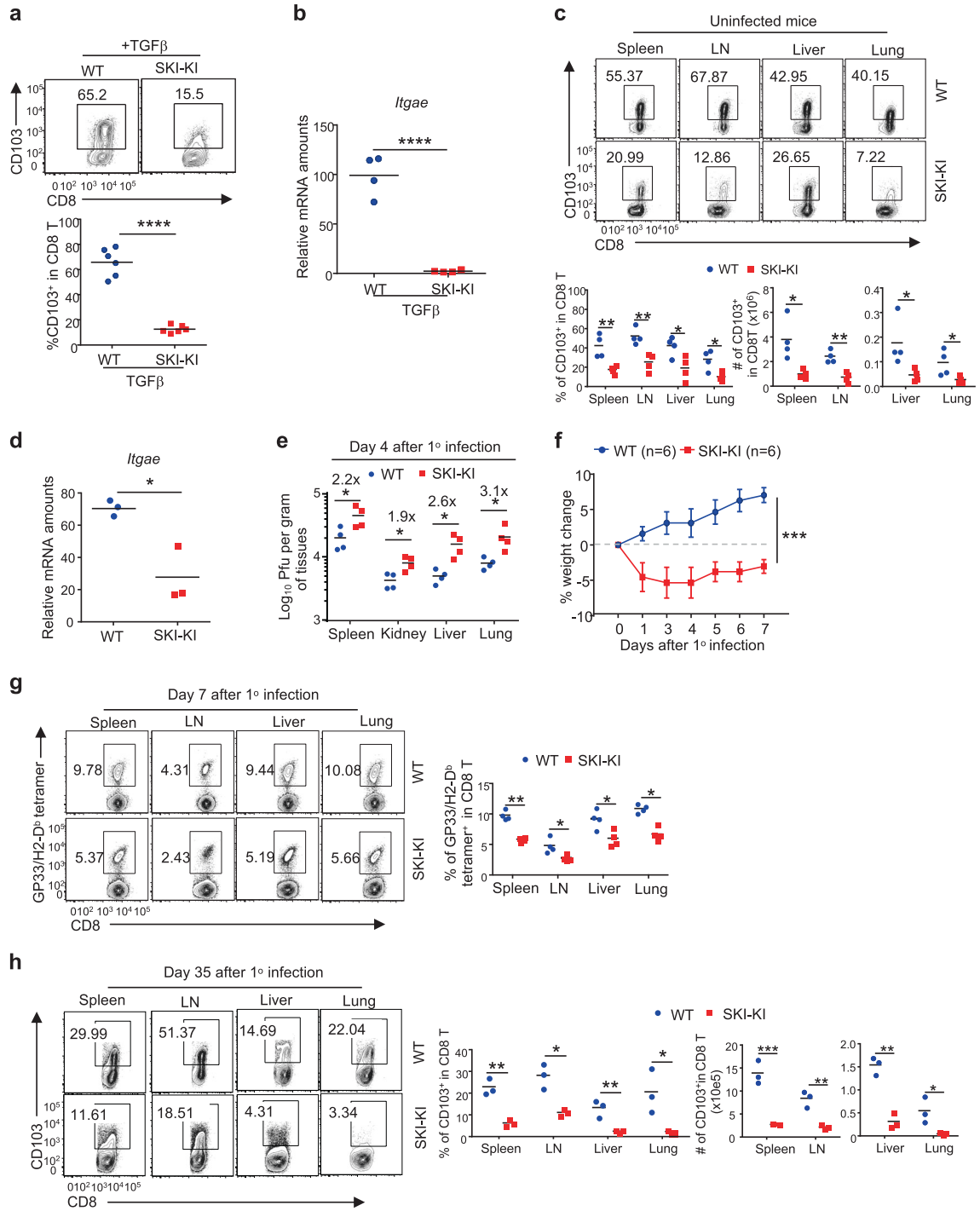

Fig. 4 SKI suppresses CD103$^+$CD8$^+$ T cell generation and dampens antiviral responses. **a** Flow cytometry of CD103 expression on CD8$^+$ T cells of the indicated genotypes after being activated in the presence of TGFβ for 2 days. ($n = 5$ samples from three experiments; representative results are shown; ***$p < 0.001$; per two-sided *t*-test; centers indicate the mean values). **b** qRT-PCR analysis of mRNA levels of *Itgae* gene-expressed CD8$^+$ T cells of the indicated genotypes after being activated in the presence of TGFβ for 2 days. ($n = 3$ mice of three experiments; **$p < 0.01$ per two-sided *t*-test; centers indicate the mean values). **c** Flow cytometry of CD103 expression on CD8$^+$ T cells from mice with the indicated genotypes to determine the percentages and numbers of CD103$^+$CD8$^+$ T cells in different tissues. ($n = 4$ mice of four experiments; representative results are shown; *$p < 0.05$, **$p < 0.01$ per two-sided *t*-test; centers indicate the mean values). **d** qRT-PCR analysis of mRNA levels of the *Itgae* gene expressed by splenic CD8$^+$ T cells isolated from mice of the indicated genotypes. ($n = 3$ mice of three experiments; *$p < 0.05$ per two-sided *t*-test; centers indicate the mean values). **e**, **f** Mice with the indicated genotypes were infected once (1°) with LCMV-Armstrong. The viral titer in different tissues (**e**) and body weight changes (**f**) were assessed at the indicated time points. ($n = 4$ mice for (**e**) and $n = 6$ mice for (**f**) of two experiments; the mean ± s.e.m. for (**f**); *$p < 0.05$ per two-sided *t*-test for (**e**); ***$p < 0.001$ per two-way multiple-range ANOVA test for (**f**); centers indicate the mean values). **g** The percentages of LCMV-specific CD8$^+$ T cells detected by GP33/H2-D^b tetramer staining and flow cytometry in mice of the indicated genotypes 7 days after LCMV infection. ($n = 4$ mice of three experiments; *$p < 0.05$, **$p < 0.01$ per two-sided *t*-test; centers indicate the mean values). **h** The percentages and numbers of CD103$^+$CD8$^+$ T cells in different tissues from mice of the indicated genotypes 35 days post LCMV-Armstrong infection, assessed by flow cytometry. ($n = 3$ mice of three experiments; *$p < 0.05$, **$p < 0.01$, and ***$p < 0.001$ per two-sided *t*-test; centers indicate the mean values)

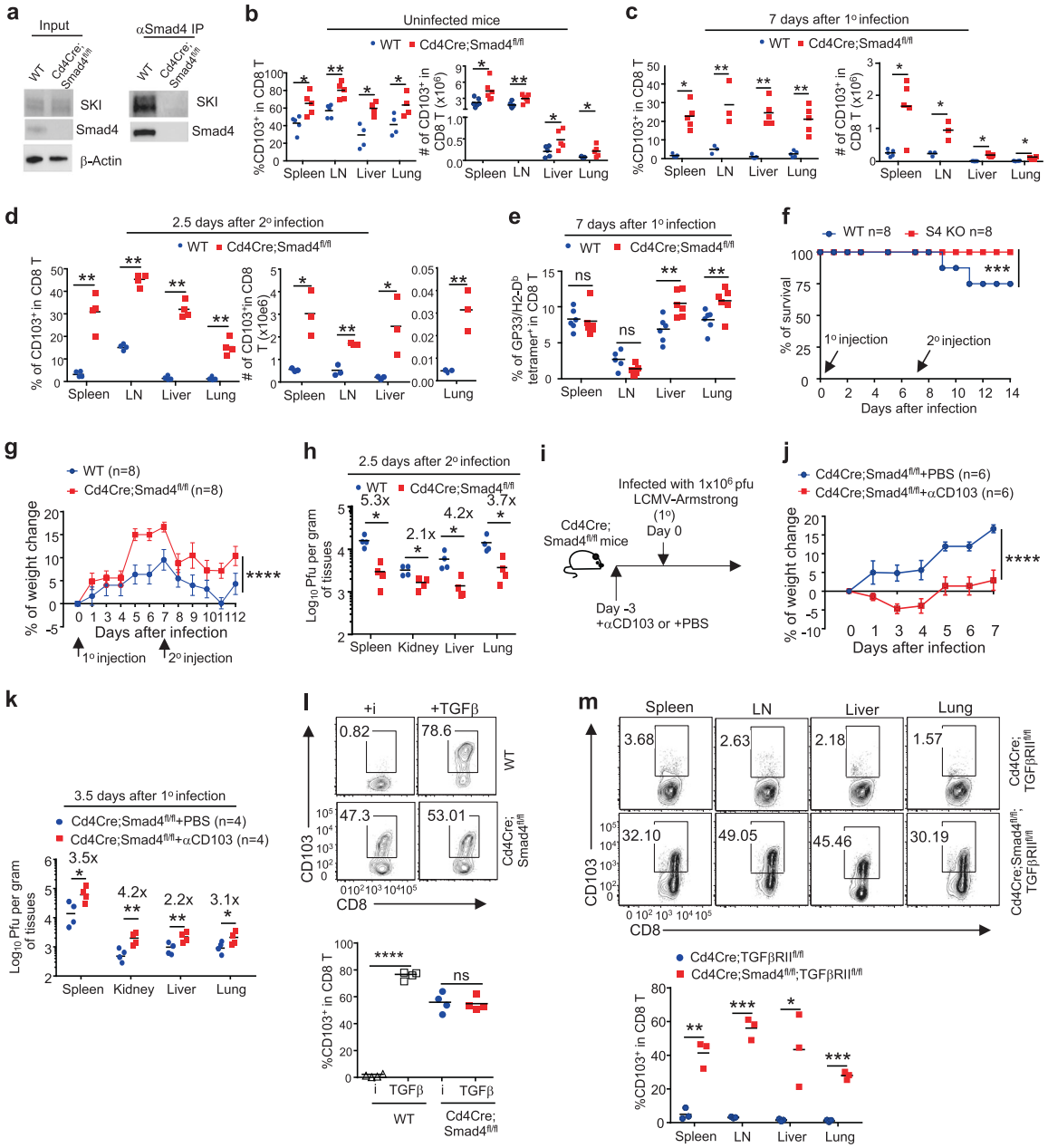

Fig. 5 Smad4 interacts with SKI and is required to suppress CD103 expression in $CD8^+$ T cells. **a** The interaction between Smad4 and SKI in $CD8^+$ T cells was detected by co-immunoprecipitation. The results are representative of three experiments. **b** The percentages and numbers of $CD103^+CD8^+$ T cells in different tissues of naïve mice with the indicated genotypes, as assessed by flow cytometry. ($n = 4$–5 mice of three experiments; $^*p < 0.05$, $^{**}p < 0.01$ per two-sided *t*-test; centers indicate the mean values). **c** The percentages and numbers of $CD103^+CD8^+$ T cells in different tissues of mice with the indicated genotypes after infection once (1°) with LCMV-Armstrong for 7 days, assessed by flow cytometry. ($n = 3$–5 mice of three experiments; $^*p < 0.05$, $^{**}p < 0.01$ per two-sided *t*-test; centers indicate the mean values). **d** The percentages and numbers of $CD103^+CD8^+$ T cells in different tissues of mice with the indicated genotypes after infection twice (2° as described in Fig. 1c) for 2.5 days, assessed by flow cytometry. ($n = 3$–4 mice of three experiments; $^*p < 0.05$, and $^{**}p < 0.01$ per two-sided *t*-test; centers indicate the mean values). **e** The percentages of LCMV-specific, GP33/H2-Db tetramer-positive $CD8^+$ T cells in different tissues of mice of the indicated genotypes after infection once (1°) with LCMV-Armstrong for 7 days, assessed by flow cytometry. ($n = 6$ mice of three experiments; ns, not significant, $^{**}p < 0.01$ per two-sided *t*-test; centers indicate the mean values) (**f**–**h**). Mice of the indicated genotypes were infected with LCMV-Armstrong twice (2°). The survival rate (**f**), change in body weight (**g**), and viral titers in different tissues (**h**) were monitored at the indicated time points. ($n = 8$ mice for (**f**, **g**) and $n = 4$ mice for (**h**) of two experiments; the mean ± s.e.m. for (**g**); $^{****}p < 0.0001$ per two-way multiple-range ANOVA test for (**f**) and (**g**); $^*p < 0.05$ per two-sided *t*-test for (**h**); centers indicate the mean values). **i** The experimental design of anti-CD103 treatment followed by LCMV-Armstrong infection as shown in (**j**–**k**). The body weight change (**j**) and viral titers in different tissues (**k**) of LCMV-infected mice of the indicated genotypes as described in (**i**). ($n = 6$ mice of two experiments for (**j**); $n = 4$ mice of two experiments for (**k**); $^{****}p < 0.0001$ per two-way multiple-range ANOVA test for (**j**); $^*p < 0.05$, $^{**}p < 0.01$ per two-sided *t*-test for (**k**); centers indicate the mean values). **l** Flow cytometry of CD103 expression by $CD8^+$ T cells of the indicated genotypes after being activated in the presence of TGFβ receptor inhibitor (i) or TGFβ. (Representative results are shown; $n = 4$ samples of three experiments; ns not significant, $^{****}p < 0.0001$ per two-sided *t*-test; centers indicate the mean values) **m** Flow cytometry of CD103 expression by $CD8^+$ T cells in different tissues from mice of the indicated genotypes. (Representative results are shown; $n = 3$ mice of three experiments, $^*p < 0.05$, $^{**}p < 0.01$, and $^{***}p < 0.001$; per two-sided *t*-test; centers indicate the mean values)

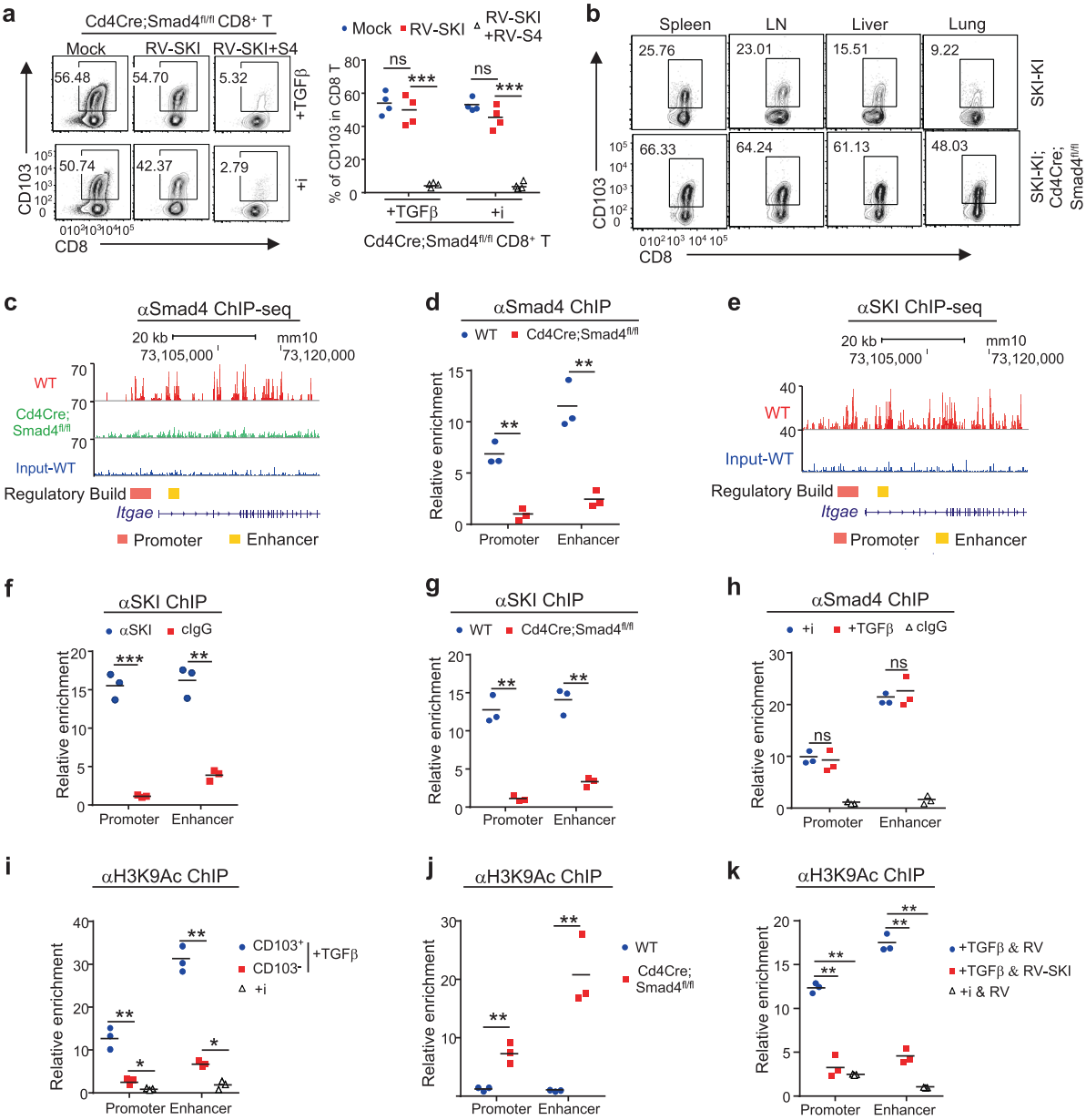

Fig. 6 SKI co-opts Smad4 to directly suppress *Itgae* transcription by inhibiting histone acetylation. **a** Smad4-deficient CD8$^+$ T cells were purified and activated in the presence of TGFβ or TGFβR inhibitor (i) and transduced with MSCV-SKI-IRES-Thy1.1 (RV-SKI) and/or MSCV-Smad4-IRES-EGFP (RV-S4), as indicated. The expression of CD103 by the transduced cells was detected by flow cytometry. (Representative results are shown. $n = 4$ samples from three experiments; ns not significant, ***$p < 0.001$ per two-sided *t*-test; centers indicate the mean values). **b** Flow cytometry of CD103 expression by CD8$^+$ T cells in different tissues from mice of the indicated genotypes. (Results are representative of three experiments). **c** Chromatin immunoprecipitation followed by sequencing (ChIP-seq) analysis of Smad4 binding at the *Itgae* loci in CD8$^+$ T cells cultured with TGFβR inhibitor for 2 days. **d** ChIP analysis of Smad4 binding at the *Itgae* promoter and enhancer regions in CD8$^+$ T cells cultured with TGFβR inhibitor for 2 days. ($n = 3$ samples of three experiments, **$p < 0.01$ per two-sided *t*-test; centers indicate the mean values). **e** ChIP-seq analysis of SKI binding at the *Itgae* locus in CD8$^+$ T cells cultured with TGFβR inhibitor for 2 days. **f** ChIP analysis of SKI binding at the *Itgae* promoter and enhancer regions in CD8$^+$ T cells cultured with TGFβR inhibitor for 2 days. cIgG (control IgG). ($n = 3$ samples of three experiments, **$p < 0.01$, and ***$p < 0.001$, per two-sided *t*-test; centers indicate the mean values) **g** ChIP analysis of SKI binding at the *Itgae* promoter and enhancer regions in activated CD8$^+$ T cells from mice with the indicated genotypes that were grown in the presence of TGFβR inhibitor for 2 days. ($n = 3$ samples of three experiments; **$p < 0.01$ per two-sided *t*-test; centers indicate the mean values). **h** ChIP analysis of Smad4 binding at the *Itgae* promoter and enhancer regions in activated CD8$^+$ T cells cultured in the presence of TGFβR inhibitor (i) or TGFβ for 2 days. cIgG (control IgG). ($n = 3$ samples of three experiments; ns, not significant per two-sided *t*-test; centers indicate the mean values). **i** CD8$^+$ T cells were purified and activated in the presence of TGFβR inhibitor (i) or TGFβ for 2 days. CD103$^+$ and CD103$^-$ subsets were sorted from TGFβ-treated CD8$^+$ T cells. H3K9 acetylation (H3K9Ac) at the *Itgae* promoter and enhancer regions was assessed by ChIP analysis. ($n = 3$ samples of three experiments, *$p < 0.05$, and **$p < 0.01$, per two-sided *t*-test; centers indicate the mean values). **j** ChIP analysis of H3K9Ac at the *Itgae* promoter and enhancer regions in CD8$^+$ T cells of the indicated genotypes 2 days after activation in the presence of a TGFβR inhibitor. ($n = 3$ samples of three experiments; **$p < 0.01$ per two-sided *t*-test; centers indicate the mean values). **k** ChIP analysis of H3K9Ac at the *Itgae* promoter and enhancer regions in MSCV-SKI-IRES-Thy1.1 (RV-SKI)- or MSCV-IRES-Thy1.1 (RV)-transduced CD8$^+$ T cells that were grown in the presence of TGFβ or TGFβR inhibitor (i). ($n = 3$ samples of three experiments, **$p < 0.01$ per two-sided *t*-test; centers indicate the mean values)

In summary, this study reveals that CD103 is expressed by $CD8^+$ T cells in lymphoid and nonlymphoid tissues. Such CD103 expression endows $CD8^+$ T cells with an optimal ability to respond to and clear pathogens. In addition, CD103 expression is regulated specifically via the TGFβ–SKI–Smad4 pathway, shedding light on the long-sought mechanisms underlying TGFβ-controlled CD103 expression in $CD8^+$ T cells. This work not only provides insights into the function and regulation of CD103 in $CD8^+$ T cells but also unveils new molecular targets for specifically modulating resident $CD103^+CD8^+$ T cell functions for pathogen clearance.

DISCUSSION

$CD103^+$ Trm $CD8^+$ cells have attracted great attention for their involvement in pathogen clearance, vaccination, and tumor immunity.[38,49,50] As a hallmark of Trm $CD8^+$ T cells, CD103 promotes the tissue migration and retention of $CD8^+$ T cells in nonlymphoid tissues.[23] Nevertheless, emerging evidence suggests that CD103 expression is not restricted to Trm $CD8^+$ T cells.[12] $CD103^+CD8^+$ T cells are easily detected in lymphoid and nonlymphoid tissues as well as in peripheral blood,[35,51,52] implying that resident $CD103^+CD8^+$ T cells may have functions in addition to those in the memory response. In this study, we provided evidence to support the notion that CD103 is important for the $CD8^+$ T cell-mediated effector response and that resident $CD103^+CD8^+$ T cells are poised to mount an optimal response towards pathogens. In light of the current finding that resident $CD103^+CD8^+$ T cells are important for controlling primary and secondary viral infection, it will be interesting to investigate how broadly this mechanism is involved in the clearance of various viral and bacterial pathogens as well as in effective vaccination.

We found that CD103 expression in $CD8^+$ T cells was dynamically regulated during viral infection. CD103 expression declined aggressively and reached the lowest level at ~7 days post infection. Considering that CD103 is important for the tissue retention of T cells,[12] the decline of its expression during the antiviral response is likely to facilitate the mobility of activated effector $CD8^+$ T cells to survey the body and clear infected cells. In agreement with this notion, strong T cell receptor (TCR) activation induces the upregulation of T-bet and Eomes to potently suppress CD103 expression.[53–56] Interestingly, we also noticed that $CD8^+$ T cells regained CD103 expression 35 days post infection when the pathogens were largely cleared.[57] Regaining CD103 expression in the absence of overt infection and strong T cell stimulation should allow pathogen-exposed migrating $CD8^+$ T cells to locate to the tissues and facilitate the formation of Trm $CD8^+$ T cells.

The expression of CD103 is controlled through multiple mechanisms,[12,24] among which TGFβ signaling is critical for promoting its expression.[25–27,58] However, the signaling pathways downstream of TGFβR in regulating CD103 expression remain poorly defined. R-Smads were activated in $CD103^+CD8^+$ T cells (Fig. 3) and are required for TGFβ-promoted CD103 expression.[27] Mechanistically, Smad2/3 and NFAT are critical transcriptional factors that directly bind the promoter and enhancer regions of *Itgae* loci and promote CD103 transcription.[58] Our data now suggest that SKI co-opts Smad4 to restrain CD103 expression by directly binding to *Itgae* loci. However, we found that R-Smads were comparably activated in $CD103^+CD8^+$ and $CD103^-CD8^+$ T cells, suggesting that an additional TGF-β-dependent mechanism beyond that of R-Smads directs CD103 expression in $CD8^+$ T cells. Indeed, we found that SKI expression specifically and inversely correlated with CD103 expression and that SKI suppressed CD103 expression. These results uncover a unique role for SKI-dependent signaling in restricting CD103 expression. We thus propose a "dual role" model for TGFβ to promote CD103 expression[1]: TGFβ activates R-Smads to potentiate CD103 transcription and[2] TGFβ triggers SKI downregulation to relieve SKI/Smad4-mediated suppression to permit CD103 transcription. Therefore, interfering with SKI function could be a viable approach to specifically target $CD8^+$ T cell function for pathogen clearance.

The current study highlights an important role for SKI in controlling CD103 expression and $CD8^+$ T cell function for viral clearance. How SKI expression and function are regulated is thus of interest. We found that SKI expression was increased in activated $CD8^+$ T cells, facilitating CD103 downregulation in these cells. Because the SKI expression level is inversely correlated with TGFβ stimulation, the increased SKI expression in activated T cells could be due to their reduced sensitivity towards TGFβ stimulation because TGFβRI expression is drastically downregulated in T cells upon activation.[59] SKI expression is regulated predominantly at a posttranslational level through modulation of protein stability. Polyubiquitination and proteasome-mediated protein degradation are important for SKI degradation.[30] One of the E3 ubiquitin ligases, Arkadia, has been shown to facilitate TGFβ-induced SKI protein degradation in nonlymphoid cells.[60] Nonetheless, whether Arkadia, other E3 ubiquitin ligase(s), and proteasomal-independent mechanisms contribute to the regulation of SKI expression in T cells warrants further investigation.

SKI functions by regulating gene transcription through epigenetic modification of gene loci.[30] Because SKI is neither a transcription factor nor an enzyme that regulates epigenetic modifications, it is imperative for SKI to co-opt-related factors to carry out its functions.[61] Indeed, we found that SKI interacted with the transcription factor Smad4, which is critical for the recruitment of SKI to the *Itgae* loci to control CD103 expression. In addition to Smad4, SKI can interact with other transcription factors, including PU.1, GATA1, and Gli3, in a cellular context-dependent manner.[30] If and how SKI functions with any of these other transcription factors to control *Itgae* expression remain to be addressed. In addition, we found that the recruitment of SKI to *Itgae* loci resulted in transcriptional repression associated with decreased histone acetylation, which can be achieved by either recruiting histone deacetylase (HDAC) or excluding histone acetyl transferase.[48] Because SKI has been shown to bind to HDAC1 and HDAC3,[62,63] it is likely that SKI suppresses *Itgae* expression by recruiting HDACs. Further investigation is therefore warranted to shed light on the precise mechanisms underlying SKI-controlled *Itgae* expression.

MATERIALS AND METHODS

Animal

Cd4Cre, Smad4$^{fl/fl}$, *Tgfbr2$^{fl/fl}$*, *Cd4Cre;Rosa26-iSki* (*SKI-KI*), and CD45.1 congenic wild-type mice were on a C57BL/6 background. Two- to four-month-old, age- and sex-matched male and female mice were used for experiments. Littermates were used unless stated otherwise. All mice were housed and bred in specific pathogen-free conditions in the animal facility at the University of North Carolina at Chapel Hill. All mouse experiments were approved by the Institutional Animal Care and Use Committee of the University of North Carolina. We have complied with all relevant ethical regulations.

Generation of Cd4Cre;Rosa26-iSki (SKI-KI) mice

The synthesized mSki-flag cDNA was ligated into the mROSA-KI-12 vector to generate the mROSA26-mSki-flag targeting vector. This cassette was inserted between the first and second exons of the safe harbor locus of Rosa26 loci by sgRosa26/Cas9-introduced double-strand break. Microinjection of the targeting vector was performed in zygotes from C57BL/6 female mice. F0 mice were bred with wild-type C57BL/6 mice to obtain F1 germline transmission heterozygous mice after validation by PCR and southern blotting. F1 germline transmitted mice were bred with *Cd4Cre* mice to generate *Cd4Cre;Rosa26-iSki* (*SKI-KI*) mice.

LCMV-Armstrong infection and in vivo antibody treatment
Mice at 8–12 weeks of age were infected intraperitoneally with LCMV-Armstrong (1×10^6 plaque-forming units, pfu). For the repeated infection model, mice were rechallenged intraperitoneally with 1×10^6 pfu LCMV-Armstrong on day 7 after the 1st. infection. *InVivoMAb* anti-mouse CD103 (M209; BioXcell) was administered intraperitoneally at a dose of 0.5 mg per mouse 3 days before LCMV-Armstrong infection.

LCMV-Armstrong propagation and titering
Viral stocks of LCMV-Armstrong were propagated from infected BHK21 cell monolayers. Virus titers in the spleen, liver, lung and kidney were determined by plaque assay on Vero cell monolayers.

Flow cytometry
T cells from various experiments were stained with the following fluorescence-labeled antibodies: anti-CD4 (RM4-5), anti-CD8 (53–6.7), anti-CD25 (PC61), anti-CD103 (2E7) (Biolegend), and anti-Foxp3 (FJK-16s) from eBioscience. The MHC class I tetramer of H-2D^b complexed with the LCMV GP33-41 peptide was obtained from the NIH tetramer core facility at Emory University. The data were acquired by FACSCanto (BD Bioscience) and were analyzed by FlowJo software (Treestar).

T cell isolation and culturing in vitro
CD8$^+$ T cells were isolated from the peripheral lymph nodes and spleens from mice by CD8 magnetic beads (Miltenyi Biotec) per the manufacturer's protocols. To isolate CD103$^+$ cells, cells were stained with a biotin-conjugated anti-mouse CD103 antibody (2E7, Biolegend) and then were purified by streptavidin magnetic beads (Miltenyi Biotec). The flow-through CD8$^+$ T cells were collected by CD8 magnetic beads (Miltenyi Biotec) to obtain CD103$^-$CD8$^+$ cells. Sorted cells were then subjected to subsequent culture and analysis. To activate purified T cells, they were cultured on plates precoated with 5 μg/ml anti-CD3 (145-2C11, BioXCell) and 2 μg/ml anti-CD28 (37.51, BioXCell) in RPMI medium supplemented with 10% FBS. TGFβ (0.25 ng/ml, Biolegend) or 10 μM TGFβR inhibitor SB525334 (Selleckchem) was added as required.

Lymphocyte isolation from nonlymphoid tissues
Lung tissues were cut into pieces and digested for 45 min with 1 mg/ml collagenase D (Sigma) in PBS at 37 °C with shaking every 15 min. Digested tissues were filtered through a 70 μm nylon cell strainer (Falcon). Lymphocytes were then separated by using a 38% Percoll (Sigma) solution with centrifugation. Liver tissues were excised and homogenized. Lymphocyte suspensions were then separated using a 40/70% Percoll density gradient with centrifugation. Lymphocytes were then extracted and subjected to subsequent analysis.

Quantitative RT-PCR (qRT-PCR) analysis
Total RNA was extracted from lymphocytes using TRIsure reagent (Bioline), and it was reverse-transcribed to generate cDNA with Superscript III reverse transcriptase (Bio-Rad) per the manufacturer's protocols. Quantitative PCR (qPCR) was performed on a QuantStudio 6 Flex Real-Time PCR System (Thermo Fisher Scientific). The housekeeping gene actin was used as an internal control for normalization of all qPCR results. Normalized qPCR results are presented as relative mRNA amounts with arbitrary units to show different levels of gene expression.

Immunoblotting and IP
For immunoblotting, protein extracts were resolved by 4–15% Mini-PROTEAN TGX Precast Protein Gels (Bio-Rad), transferred to a polyvinylidene fluoride membrane (Bio-Rad) and analyzed by immunoblotting with the following antibodies: anti-SKI (G8, Santa Cruz), anti-Smad4 (D3M6U, CST), anti-β-actin (C4, Santa Cruz), anti-phospho-Smad2 (S465/467, CST), anti-phospho-Smad3 (C25A9, CST), anti-Smad2 (D43B4, CST), and anti-Smad3 (C67H9, CST).

For IP, cells were lysed with IP lysis buffer (10 mM HEPES, pH 7.5, 1.5 mM $MgCl_2$, 0.2 mM EDTA, and 150 mM NaCl containing 1% NP40) containing a protease inhibitor mixture (Roche Applied Science), and then they were sonicated with Bioruptor PICO. Cell lysates were incubated with 50 μl of magnetic protein A/G beads (Bio-Rad) that had been conjugated to the indicated antibodies and treated with dimethyl pimelimidate. After overnight incubation, the associated protein was eluted with 2 × Laemmli sample buffer (Bio-Rad) after five washes and incubated at 95 °C for 5 min. Then, the eluted samples were separated by SDS-PAGE and analyzed by immunoblotting.

Retroviral transduction
For retroviral transduction, CD8$^+$ T cells were isolated and cultured under various conditions and then spin-inoculated (at $1500 \times g$) with the indicated MSCV retroviruses in the presence of 8 μg/ml polybrene (Sigma-Aldrich) and HEPES buffer (Gibco) at 30 °C for 90 min 24 h after activation. Transduced cells were harvested and analyzed by flow cytometry.

ChIP assay
Isolated CD8$^+$ T cells were cross-linked with 1% formaldehyde (Sigma) and lysed in lysis buffer. Lysates were sonicated with Bioruptor PICO to shear genomic DNA. Chromatin was then subjected to immunoprecipitation overnight at 4 °C with anti-Smad4 (EP618Y, Abcam), anti-Ski (G8, Santa Cruz), anti-H3K9Ac (ab4441, Abcam), normal mouse IgG (sc-2025, Santa Cruz), and normal rabbit IgG (sc-2027, Santa Cruz). qPCR was performed to detect the relative abundance of the target genomic DNA. Specific PCR primers to detect the *Itgae* promoter and enhancer region (predicted by ENCODE) are as follows: promoter: CTCCTAGGGAG CAGGTGTCT and TAGAAAAGCCTGCACGGGAT; enhancer: GGTA CATGGAAGCCTGAGCA and AGACAGAGGGCCTAAGAGCA.

ChIP-seq
The sequencing libraries were prepared with an MGI Easy DNAseq kit (MGI), and sequence data were collected using 50 nt single-end reads with a BGISEQ-500 system (MGI) at the BGI Genomics company. Raw reads (24–25 million reads per sample) were first processed to remove adapter sequences using Trim Galore (version 0.4) with default parameters. The resulting reads were aligned to mm10 using Bowtie (version 1.2) with the parameters -m 1, -v 2, and -X 1500. These parameters ensured that fragments that were up to 1500 bp (-X 1500) with mismatches of up to 2 (-v 2) were allowed to align and that only unique aligning reads were collected (-m 1). For all the data files, duplicated alignments were removed using Picard (version 1.115). The ChIP-seq data are available in the Gene Expression Omnibus repository at the National Center for Biotechnology Information under accession number GSE135533.

The findPeaks program from Homer (version 4.8.3) was applied to call all reported ChIP-seq peaks. The basic goal was to identify regions in the genome where more sequencing reads could be found than would be expected by chance. Peak calling for all samples used the paired input sample as noise control. The findPeaks program was run using default parameters of "-F 4 -L 0 -C 2 -fdr 0.001". "-F" required each putative peak to have fourfold more normalized tags in the target experiment than the control. "-L 0" disabled the local signal. "-C 2" was used to remove peaks near repeat elements that contain odd tag distributions. "-fdr 0.001" indicated that FDR-adjusted p value < 0.05 was used as cutoff. All significant peaks were associated with genes using GREAT (Version 3).

Statistical analysis
A Student's t test or two-way ANOVA was used for two-group comparisons. p values of < 0.05 were considered significant. In the figures, *, **, *** and **** were used to indicate $p < 0.05$, $p < 0.01$,

$p < 0.001$ and $p < 0.0001$, respectively. All results shown are the mean ± s.d. unless otherwise stated.

DATA AVAILABILITY

ChIP-seq data are deposited in the GEO database under ID code GSE135533.

ACKNOWLEDGEMENTS

We thank E. Robertson and E. Bikoff for providing *Smad4*$^{fl/fl}$ mice, H. Moses for providing *Tgfbrll*$^{fl/fl}$ mice, and the NIH tetramer core facility at Emory University for providing the tetramers. This work was supported by NIH funding (R01AI143894; R01AI138337) for J.K.W.; the NIH (AI123193); the National Multiple Sclerosis Society (RG-1802-30483); and the Yang Family Biomedical Scholars Award for Y.Y.W.

AUTHOR CONTRIBUTIONS

B.W. and G.Z. contributed equally to the design and implementation of the cellular, molecular, biochemical, and animal experiments; B.W. contributed to the writing of the manuscript; Z.G., G.W., and J. Z. contributed to the generation and characterization of *SKI-KI* mice; J.L. and X.X. contributed to the bioinformatic analysis of ChIP data; J.K.W. contributed to the LCMV infection model; and Y.Y.W. conceived the project, designed the experiments, and wrote the manuscript.

ADDITIONAL INFORMATION

The online version of this article (https://doi.org/10.1038/s41423-020-0495-7) contains supplementary material.

Competing interests: The authors declare no competing interests.

REFERENCES

1. Rynda-Apple, A., Robinson, K. M. & Alcorn, J. F. Influenza and bacterial superinfection: illuminating the immunologic mechanisms of disease. *Infect. Immun.* **83**, 3764–3770 (2015).
2. van der Sluijs, K. F. et al. IL-10 is an important mediator of the enhanced susceptibility to pneumococcal pneumonia after influenza infection. *J. Immunol.* **172**, 7603–7609 (2004).
3. Brundage, J. F. Interactions between influenza and bacterial respiratory pathogens: implications for pandemic preparedness. *Lancet Infect. Dis.* **6**, 303–312 (2006).
4. Paget, C. & Trottein, F. Mechanisms of bacterial superinfection post-influenza: a role for unconventional T cells. *Front. Immunol.* **10**, 336 (2019).
5. Ivanov, S. et al. Key role for respiratory CD103(+) dendritic cells, IFN-gamma, and IL-17 in protection against Streptococcus pneumoniae infection in response to alpha-galactosylceramide. *J. Infect. Dis.* **206**, 723–734 (2012).
6. Wong, P. & Pamer, E. G. CD8 T cell responses to infectious pathogens. *Annu. Rev. Immunol.* **21**, 29–70 (2003).
7. Restifo, N. P., Dudley, M. E. & Rosenberg, S. A. Adoptive immunotherapy for cancer: harnessing the T cell response. *Nat. Rev. Immunol.* **12**, 269–281 (2012).
8. Chang, J. T., Wherry, E. J. & Goldrath, A. W. Molecular regulation of effector and memory T cell differentiation. *Nat. Immunol.* **15**, 1104–1115 (2014).
9. Gebhardt, T. et al. Memory T cells in nonlymphoid tissue that provide enhanced local immunity during infection with herpes simplex virus. *Nat. Immunol.* **10**, 524–530 (2009).
10. Cepek, K. L. et al. Adhesion between epithelial cells and T lymphocytes mediated by E-cadherin and the alpha E beta 7 integrin. *Nature* **372**, 190–193 (1994).
11. Iijima, N. & Iwasaki, A. Tissue instruction for migration and retention of TRM cells. *Trends Immunol.* **36**, 556–564 (2015).
12. Hardenberg, J. B., Braun, A. & Schon, M. P. A Yin and Yang in epithelial immunology: the roles of the alphaE(CD103)beta7 Integrin in T Cells. *J. investig. Dermatol.* **138**, 23–31 (2018).
13. Schlickum, S. et al. Integrin alpha E(CD103)beta 7 influences cellular shape and motility in a ligand-dependent fashion. *Blood* **112**, 619–625 (2008).
14. Smazynski, J. & Webb, J. R. Resident memory-like tumor-infiltrating lymphocytes (TILRM): latest players in the immuno-oncology repertoire. *Front. Immunol.* **9**, 1741 (2018).
15. Annacker, O. et al. Essential role for CD103 in the T cell-mediated regulation of experimental colitis. *J. Exp. Med.* **202**, 1051–1061 (2005).
16. Duhen, T. et al. Co-expression of CD39 and CD103 identifies tumor-reactive CD8 T cells in human solid tumors. *Nat. Commun.* **9**, 2724 (2018).
17. Gabriely G. et al. Targeting latency-associated peptide promotes antitumor immunity. *Sci. Immunol.* **2**, eaaj1738 (2017).
18. Shields, B. D. et al. Loss of E-cadherin inhibits CD103 antitumor activity and reduces checkpoint blockade responsiveness in melanoma. *Cancer Res.* **79**, 1113–1123 (2019).
19. Boutet, M. et al. TGFbeta signaling intersects with CD103 integrin signaling to promote T-lymphocyte accumulation and antitumor activity in the lung tumor microenvironment. *Cancer Res.* **76**, 1757–1769 (2016).
20. Abd Hamid, M. et al. Self-maintaining CD103(+) cancer-specific T cells are highly energetic with rapid cytotoxic and effector responses. *Cancer Immunol. Res.* **8**, 203–216 (2020).
21. Franciszkiewicz, K. et al. CD103 or LFA-1 engagement at the immune synapse between cytotoxic T cells and tumor cells promotes maturation and regulates T-cell effector functions. *Cancer Res.* **73**, 617–628 (2013).
22. Xue, D., Liu, P., Chen, W., Zhang, C. & Zhang, L. An anti-CD103 antibody-drug conjugate prolongs the survival of pancreatic islet allografts in mice. *Cell Death Dis.* **10**, 735 (2019).
23. Hadley, G. A. & Higgins, J. M. Integrin alphaEbeta7: molecular features and functional significance in the immune system. *Adv. Exp. Med. Biol.* **819**, 97–110 (2014).
24. Milner, J. J. & Goldrath, A. W. Transcriptional programming of tissue-resident memory CD8(+) T cells. *Curr. Opin. Immunol.* **51**, 162–169 (2018).
25. Zhang, N. & Bevan, M. J. Transforming growth factor-beta signaling controls the formation and maintenance of gut-resident memory T cells by regulating migration and retention. *Immunity* **39**, 687–696 (2013).
26. El-Asady, R. et al. TGF-{beta}-dependent CD103 expression by CD8(+) T cells promotes selective destruction of the host intestinal epithelium during graft-versus-host disease. *J. Exp. Med.* **201**, 1647–1657 (2005).
27. Takimoto, T. et al. Smad2 and Smad3 are redundantly essential for the TGF-beta-mediated regulation of regulatory T plasticity and Th1 development. *J. Immunol.* **185**, 842–855 (2010).
28. Li, M. O., Wan, Y. Y., Sanjabi, S., Robertson, A. K. & Flavell, R. A. Transforming growth factor-beta regulation of immune responses. *Annu. Rev. Immunol.* **24**, 99–146 (2006).
29. Sun, Y., Liu, X., Ng-Eaton, E., Lodish, H. F. & Weinberg, R. A. SnoN and Ski protooncoproteins are rapidly degraded in response to transforming growth factor beta signaling. *Proc. Natl Acad. Sci. USA* **96**, 12442–12447 (1999).
30. Deheuninck, J. & Luo, K. Ski and SnoN, potent negative regulators of TGF-beta signaling. *Cell Res.* **19**, 47–57 (2009).
31. Bonthius, D. J. Lymphocytic choriomeningitis virus: an underrecognized cause of neurologic disease in the fetus, child, and adult. *Semin Pediatr. Neurol.* **19**, 89–95 (2012).
32. Zhou, X., Ramachandran, S., Mann, M. & Popkin, D. L. Role of lymphocytic choriomeningitis virus (LCMV) in understanding viral immunology: past, present and future. *Viruses* **4**, 2650–2669 (2012).
33. Grueter, B. et al. Runx3 regulates integrin alpha E/CD103 and CD4 expression during development of CD4-/CD8+ T cells. *J. Immunol.* **175**, 1694–1705 (2005).
34. Andrew, D. P., Rott, L. S., Kilshaw, P. J. & Butcher, E. C. Distribution of alpha 4 beta 7 and alpha E beta 7 integrins on thymocytes, intestinal epithelial lymphocytes and peripheral lymphocytes. *Eur. J. Immunol.* **26**, 897–905 (1996).
35. Fousteri, G. et al. Minimal effect of CD103 expression on the control of a chronic antiviral immune response. *Viral Immunol.* **23**, 285–294 (2010).
36. Dutko, F. J. & Oldstone, M. B. Genomic and biological variation among commonly used lymphocytic choriomeningitis virus strains. *J. Gen. Virol.* **64**(Pt 8), 1689–1698 (1983).
37. Murali-Krishna, K. et al. Counting antigen-specific CD8 T cells: a reevaluation of bystander activation during viral infection. *Immunity* **8**, 177–187 (1998).
38. Mackay, L. K. et al. The developmental pathway for CD103(+)CD8+ tissue-resident memory T cells of skin. *Nat. Immunol.* **14**, 1294–1301 (2013).
39. Chytil, A., Magnuson, M. A., Wright, C. V. & Moses, H. L. Conditional inactivation of the TGF-beta type II receptor using Cre:Lox. *Genesis* **32**, 73–75 (2002).
40. Lee, P. P. et al. A critical role for Dnmt1 and DNA methylation in T cell development, function, and survival. *Immunity* **15**, 763–774 (2001).
41. Akiyoshi, S. et al. c-Ski acts as a transcriptional co-repressor in transforming growth factor-beta signaling through interaction with smads. *J. Biol. Chem.* **274**, 35269–35277 (1999).
42. Li, M. O., Sanjabi, S. & Flavell, R. A. Transforming growth factor-beta controls development, homeostasis, and tolerance of T cells by regulatory T cell-dependent and -independent mechanisms. *Immunity* **25**, 455–471 (2006).
43. Marie, J. C., Liggitt, D. & Rudensky, A. Y. Cellular mechanisms of fatal early-onset autoimmunity in mice with the T cell-specific targeting of transforming growth factor-beta receptor. *Immunity* **25**, 441–454 (2006).
44. Liu, Y. et al. A critical function for TGF-beta signaling in the development of natural CD4+CD25+Foxp3+ regulatory T cells. *Nat. Immunol.* **9**, 632–640 (2008).

45. Gu, A. D., Wang, Y., Lin, L., Zhang, S. S. & Wan, Y. Y. Requirements of transcription factor Smad-dependent and -independent TGF-beta signaling to control discrete T-cell functions. *Proc. Natl Acad. Sci. USA* **109**, 905–910 (2012).
46. Zhang, S. et al. Reversing SKI-SMAD4-mediated suppression is essential for TH17 cell differentiation. *Nature* **551**, 105–109 (2017).
47. Chu, G. C., Dunn, N. R., Anderson, D. C., Oxburgh, L. & Robertson, E. J. Differential requirements for Smad4 in TGFbeta-dependent patterning of the early mouse embryo. *Development* **131**, 3501–3512 (2004).
48. Wang, Z. et al. Genome-wide mapping of HATs and HDACs reveals distinct functions in active and inactive genes. *Cell* **138**, 1019–1031 (2009).
49. Amsen, D., van Gisbergen, K., Hombrink, P. & van Lier, R. A. W. Tissue-resident memory T cells at the center of immunity to solid tumors. *Nat. Immunol.* **19**, 538–546 (2018).
50. Park, C. O. & Kupper, T. S. The emerging role of resident memory T cells in protective immunity and inflammatory disease. *Nat. Med.* **21**, 688–697 (2015).
51. Woon, H. G. et al. Compartmentalization of total and virus-specific tissue-resident memory CD8+ T cells in human lymphoid organs. *PLoS Pathog.* **12**, e1005799 (2016).
52. Sathaliyawala, T. et al. Distribution and compartmentalization of human circulating and tissue-resident memory T cell subsets. *Immunity* **38**, 187–197 (2013).
53. Laidlaw, B. J. et al. CD4+ T cell help guides formation of CD103+ lung-resident memory CD8+ T cells during influenza viral infection. *Immunity* **41**, 633–645 (2014).
54. Mackay, L. K. et al. T-box transcription factors combine with the cytokines TGF-beta and IL-15 to control tissue-resident memory T cell fate. *Immunity* **43**, 1101–1111 (2015).
55. Pearce, E. L. et al. Control of effector CD8+ T cell function by the transcription factor eomesodermin. *Science* **302**, 1041–1043 (2003).
56. Sullivan, B. M., Juedes, A., Szabo, S. J., von Herrath, M. & Glimcher, L. H. Antigen-driven effector CD8 T cell function regulated by T-bet. *Proc. Natl Acad. Sci. USA* **100**, 15818–15823 (2003).
57. Kaech, S. M. & Cui, W. Transcriptional control of effector and memory CD8+ T cell differentiation. *Nat. Rev. Immunol.* **12**, 749–761 (2012).
58. Mokrani, M., Klibi, J., Bluteau, D., Bismuth, G. & Mami-Chouaib, F. Smad and NFAT pathways cooperate to induce CD103 expression in human CD8 T lymphocytes. *J. Immunol.* **192**, 2471–2479 (2014).
59. Tu, E. et al. T cell receptor-regulated TGF-beta type I receptor expression determines T cell quiescence and activation. *Immunity* **48**, e746 (2018).
60. Nagano, Y. et al. Arkadia induces degradation of SnoN and c-Ski to enhance transforming growth factor-beta signaling. *J. Biol. Chem.* **282**, 20492–20501 (2007).
61. Tecalco-Cruz, A. C., Rios-Lopez, D. G., Vazquez-Victorio, G., Rosales-Alvarez, R. E. & Macias-Silva, M. Transcriptional cofactors Ski and SnoN are major regulators of the TGF-beta/Smad signaling pathway in health and disease. *Signal Transduct. Target. Ther.* **3**, 15 (2018).
62. Nomura, T. et al. Ski is a component of the histone deacetylase complex required for transcriptional repression by Mad and thyroid hormone receptor. *Genes Dev.* **13**, 412–423 (1999).
63. Tabata, T., Kokura, K., Ten Dijke, P. & Ishii, S. Ski co-repressor complexes maintain the basal repressed state of the TGF-beta target gene, SMAD7, via HDAC3 and PRMT5. *Genes Cells* **14**, 17–28 (2009).